[Editor Portal] [My Manuscript Overview]
[My Manuscript Archives]

Editor
Copernicus Office

Report #1

Submitted on 11 Jan 2018
Anonymous Referee #3

Anonymous during peer-review: Yes No
Anonymous in acknowledgements of published article: Yes No

Recommendation to the editor

1) Scientific significance
Does the manuscript represent a substantial contribution to scientific progress within the scope of this journal (substantial new concepts, ideas, methods, or data)?
Excellent **Good** Fair Poor

2) Scientific quality
Are the scientific approaches and applied methods valid? Are the results discussed in an appropriate and balanced way (consideration of related work, including appropriate references)?
Excellent Good **Fair** Poor

3) Presentation quality
Are the scientific results and conclusions presented in a clear, concise, and well structured way (number and quality of figures/tables, appropriate use of English language)?
Excellent Good **Fair** Poor

For final publication, the manuscript should be

accepted as is

accepted subject to technical corrections

accepted subject to **minor revisions**

reconsidered after **major revisions**

I would like to review the revised paper.

I am **not** willing to review the revised paper.

rejected

Suggestions for revision or reasons for rejection (will be published if the paper is accepted for final publication)

We thank the anonymous reviewer for his comments.

The paper is basically acceptable but needs careful proofreading to eliminate unnecessary mistakes. For example:
P4 11, 880 km^2, not 880 km. Also 560 km^2. See also, caption to Figure 1. That's confusing—two of three reviewers note that the square is not there. However, in my original version of the manuscript I submitted, it appears.
P10, 26. Table 1, not Table 2. Thanks, changed

[Editor Portal] [My Manuscript Overview]
[My Manuscript Archives]

Editor
Copernicus Office

Report #2

Submitted on 15 Jan 2018
Anonymous Referee #1

Anonymous during peer-review: Yes No
Anonymous in acknowledgements of published article: Yes No

Recommendation to the editor

1) Scientific significance
Does the manuscript represent a substantial contribution to scientific progress within the scope of this journal (substantial new concepts, ideas, methods, or data)?
Excellent **Good** Fair Poor

2) Scientific quality
Are the scientific approaches and applied methods valid? Are the results discussed in an appropriate and balanced way (consideration of related work, including appropriate references)?
Excellent Good Fair Poor

3) Presentation quality
Are the scientific results and conclusions presented in a clear, concise, and well structured way (number and quality of figures/tables, appropriate use of English language)?
Excellent Good Fair Poor

For final publication, the manuscript should be
accepted as is
accepted subject to technical corrections
accepted subject to **minor revisions**
reconsidered after **major revisions**
I would like to review the revised paper.
I am **not** willing to review the revised paper.
rejected

Suggestions for revision or reasons for rejection (will be published if the paper is accepted for final publication)

The paper has been clearly improved. Thank you for clarifying some points and accommodating for my suggestions. I still have a few minor edits:

We thank the reviewer for his comments.

p.2 l.18: introduced Thanks, changed
l.20: 100s m. I changed it to “in the order of some kilometres to a few 100s m” since Hannawald et al. (2016) and Sedlak et al (2016) address these two ranges. These orders of magnitude are still much smaller than the one addressed by Wachter et al. (2015), which is mentioned in the sentences before and to which Hannawald et al. (2016) and Sedlak et al (2016) are compared.
p.11 l.6: remove one (Thanks, changed
p.12 l.1: data base I learned from another reviewer some time ago that it should be basis and not base (since base is something like a fundament, so something concrete, basis is something abstract). But who is right? Anyway, I am open for any improvements of my English.
p.13 p.13 l.7: 19-20 km Thanks, changed

Figure 1: ...in 4 different directions... are larger (880 km2)... Thanks, changed

Copernicus Office Editor

Report #3

Submitted on 15 Jan 2018
Referee #2: Alan Liu, liuz2@erau.edu

Anonymous during peer-review: Yes **No** **Anonymous in acknowledgements of published article:** **Yes** No

Recommendation to the editor

1) Scientific significance
Does the manuscript represent a substantial contribution to scientific progress within the scope of this journal (substantial new concepts, ideas, methods, or data)?
Excellent **Good** Fair Poor

2) Scientific quality
Are the scientific approaches and applied methods valid? Are the results discussed in an appropriate and balanced way (consideration of related work, including appropriate references)?
Excellent Good **Fair** Poor

3) Presentation quality
Are the scientific results and conclusions presented in a clear, concise, and well structured way (number and quality of figures/tables, appropriate use of English language)?
Excellent **Good** Fair Poor

For final publication, the manuscript should be

accepted as is

accepted subject to **technical corrections** accepted subject to **minor revisions** **reconsidered after major revisions**

I would like to review the revised paper.

I am **not** willing to review the revised paper.

rejected

Suggestions for revision or reasons for rejection (will be published if the paper is accepted for final publication)

Review

This revised manuscript is improved from the first version. However, I still have some major concerns, with both how the results are presented, and how the analysis was done. In the following, I provided comments following the sequence of the manuscript, with major ones marked by '*'. I also commented to the authors' replies to my first review at the end.

We appreciate the valuable comments of Alan Liu. In the following, we answered all of them and changed the manuscript accordingly where needed.

* P2, L5-10: I understand that the authors try to state the different strengths of different instruments, but they are not described accurately. There needs to be a distinction between what parameters an instrument can directly measure or sensitive to, and what parameters can be derived or 'investigated' from the measurements. For example, lidars can measure vertical profiles so can directly measure vertical variations and provide vertical wavelength. But they can also be used to derive horizontal wavelength (e.g. as in Hu et al. 2002, Lu et al. 2009, Chen et al. 2013) for inertia-gravity waves. Airglow images can directly measure horizontal wavelength but can also be used to derive vertical wavelength when background horizontal wind. The main message here is that with enough known parameters, any instrument can be used to derive other missing gravity wave parameters. The distinctions among different instruments should be what they can directly measure, not what they can be used to derive. I re-formulated this passage.

* P2, L24-26: The real 'first time' here is only about deriving vertical wavelength. Mixing them with 'zonal, meridional' wavelengths is a bit misleading. As referenced by the authors, Wachter et al. (2015) have already shown the technique of deriving horizontal wavelength. Furthermore, as I pointed in the first review, the ability to derive vertical wavelength is partially contributable to the

spatial information resolved by the scanning spectrometer (not new) and partially contributable to the horizontal wind from a nearby meteor radar (not this instrument). I suggest changing the title to 'Derivation of gravity wave intrinsic parameters and vertical wavelength using a single scanning ...' Deriving intrinsic parameters (which the vertical wavelength depends on) using a single spectrometer is really the main contribution, not the horizontal wavelength.

I agree and changed the title. I also re-formulated this passage slightly in order to emphasize the reviewer's point.

P2, L5, 'sensitive for' -> 'sensitive to' Thanks
P2, L12, 'exclusively' -> 'only'. 'Exclusively' means no other instrument can do it. Thanks, but I changed the paragraph and exclusively is not used any more
P2, L30, Wave vector is always related to intrinsic wave frequency, not just for low- and medium-frequency waves. Changed

P4, L11-12: missing the squares after 'km' You mean after 880 and 560? But there are squares in my version, also in the pdf, I just checked it.
P4, L14-15: provide an estimated uncertainty of the 5 min averaged data Done

P5, L25-27: The sentence 'The radar delivers ...' describes only a very small part of the whole procedure of meteor radar wind retrieval. The main procedure is a fitting of all radial winds within a time-altitude bin in a least-square sense, assuming homogeneity within the bin. Since 'fit' and 'fitting technique' are mentioned in subsequent sentences, what the fit means need to be described first. We changed this paragraph in order to make the procedure clearer and corrected an inaccuracy: the height gates refer to 4 km and not to 3 km. We apologize for that.

P6, L6: 'dynamical' -> 'dynamically' Thanks

* P8, L17-18: Even if the uncertainty of ground frequency is negligible, the intrinsic frequency may be not, because the latter depends on the wind in the direction of wave propagation. This Doppler wind depends on both the magnitude and direction of the background wind as well as the direction of the wave. In the analysis, the uncertainty in k and l are considered, but its indirect effect on the wave direction thus the component of the background wind in the direction of propagation is not. Please address this source of uncertainty.
I agree that the error of the intrinsic frequency may not be negligible since k, l, u, and v are probably not exact. However, when calculating the error of λ_z, we do this by taking into account the error of k, l, u, and v and the contribution of the respective variable to formula (2). This also includes the influence of these variables on the intrinsic frequency. Therefore, we take into account the error of the intrinsic frequency.

P9, L2: It's not clear what 'too conservative' means. Does it mean the 10% is an underestimate or overestimate? Please clarify. We mean that the uncertainty of 10% might be too high, so overestimated. In Wüst et al. (2017b), we calculated a "climatology" of the Brunt-Vaisala frequency over the Alpine region based on 14 years of TIMED-SABER measurements and adapted a combination of three sinusoidals to the data. This mean curve allows to calculate the Brunt-Vaisala value for every day. Ca. 98% of the Brunt-Vaisala values (for each day of the year) are located in a ±10%-interval around this mean curve. Since this interval comprises nearly all values and the variability is reduced in autumn and winter (a time period which we also address here), 10% might be too high.

P10,
L5-6: Please clarify if this phase velocity is relative to the ground or intrinsic. Also, clarify in Figure 2b and its caption. It's the velocity relative to the ground → clarified
L21-22: I don't understand why the authors say 'no vertical ... profile is suitable' first and then 'more than one is available'. Please clarify. The sentences were changed into "Depending on the orbit of TIMED, it can happen that no vertical temperature profile is suitable one day. However, the other day also more than one profile can be available."
L23: 'In one case' -> shouldn't it be 'In some cases'? There seem to be 31-19=12 cases that are without wind. The given numbers are correct, it is more a formulation problem. As said above, SABER data are not always available. In these cases, we didn't calculate the vertical wavelengths. I changed the sentence referring to the SABER data and hope that the main message is now clear. However, I am open for improvements.
L24: 'referring to' -> 'on' I can change it but I have a question before: I am only used to the article "to" in combination with "refer". I just looked it up once again in the two most common English-German web-dictionaries and in the Oxford dictionary, everywhere "refer" is used together with "to". When do I use it with "on"?

P7, L9-12: I think it's important to point out that this method looks for a single oscillation throughout an entire night (according to Wachter et al. 2015). If that's not the case, then the duration of each wave event should be given. Readers normally assume that a wave event could occur during part of a night but not the entire night, as I did at first.
We added the information that the oscillation needs to present throughout the whole night.

P10, L25-26: If I understand correctly, the authors used one detected wave from the airglow and applied multiple nearby SABER profiles and corresponding winds to obtain multiple vertical wavelengths. That's correct. This needs to be clarified in the text. Done (page 10, line 24–28). It's also not clear whether all SABER data selected are within that time period. The spatial range is described in P5L3 but not the temporal range. Information about the temporal range is now provided on page 5, lines 4–7.

P11, L3: 'table 2' should 'Table 1'. It appears the authors have deleted Table 2. That's correct, thank you
P11, L4: evanescent waves are not necessarily damped. I deleted damped.
P11, L21: Are there always 'Two wavelengths' in a SABER profile? Table 1 shows some SABER vertical wavelengths are over 15 km, which means there can only be one wavelength in the 60-80 km range. The algorithms was programmed that way that it always searched for two wavelengths and in all cases two wavelengths were identified. The given wavelength is the one which agrees best with the wavelengths derived from the GRIPS-radar combination. The procedure is explained on page 11, second half of the page. We added the information that only the value which agrees best is mentioned in table 1 (p.11, line 34).

* P11, L23-26: As the authors stated, SABER is sensitive only to oscillations with long horizontal wavelength. In Table 1, there are two cases (DOY 212 and 215) where the horizontal wavelength is only 200 km. It's true that SABER may be seeing at a horizontal angle not perpendicular to the wavefront, therefore the cancellation effect is not severe. This is however only a speculation but it can be easily demonstrated by additional analysis. Since both the wave direction and the direction of SABER sounding profile are known, their relative angles can be calculated to examine whether this speculation is correct. This needs to be done to verify if that's indeed the case.
I calculated the difference in longitude and latitude of two SABER profiles (at 86 km height) which were measured successively at DoY 212 and 215. So, one gets information about the flight direction of TIMED. The SABER instrument looks perpendicular to the flight direction. It can deliver information in the ascending and descending branch.
As long as SABER is in the same yaw cycle, its field of view can be oriented only in two ways at each latitude. With respect to the North, the absolute values are identical.
For our two examples, SABER is flying at an azimuth angle of -67° (at ca. 45°N) and 74° (at ca. 48°N). That means the fields of view are oriented mainly north-southward (23° and -16°).
On DoY 212, the wave fronts are moving at an azimuth angle of 77° +/- 10° (with respect to the North, clockwise). That means the wave fronts are mainly oriented northward (187° +/- 10°).
On DoY 215, the wave fronts are moving at an azimuth angle of 299° +/- 14°. That means the wave fronts are also mainly oriented northward (389° +/- 14° = 29° +/- 14°).
So, in both cases SABER is not measuring perpendicular to the wave fronts. In the worst case, the angle is ca. 45°.

P24: Table 1 caption should state that the period is 'ground-based.' as one reviewer asked. Adding a small subscript in the variable in the table header is not obvious to the readers. Changed

P25: Table 1 should list the intrinsic wave periods. In the manuscript, as it is, there is no information at all about the background wind and its effect. For this reason, at least the intrinsic period (and/or wind in the direction of the wave, intrinsic frequency) is necessary. Another column needed is the percentage uncertainties of airglow vertical wavelength as shown in Figure 3b. The figure only shows the distributions but one cannot tell which uncertainty is for which wavelength. Done.

Figure 1: Adding Figure 1 helps a lot. In the caption, the square after km is also missing. In my version, it is there. However, also one other review mentions this issue. Since the area of the zenith square is given, it seems natural to also give the area of the off-zenith areas in the caption. Done.

Comments to the authors' replies: Regarding the tidal effect:
The effects of tide are not about affecting different FOV differently, but about changing the assumed 86 km altitude of OH airglow. This has two effects on the derive vertical wavelength. One is changing the assumed distance between different FOVs, therefore, the derived horizontal wavelength. This error depends on the horizontal wavelength (the shorter the larger the error).
If the altitude of the FoV is changed by the same constant and not by an individually varying one (as discussed in review 1), this should not affect our results.
We measure the temperatures $T_1(x_1, y_1, z_1)$ and $T_2(x_2, y_2, z_2)$ at two different FoV.
We assume $T_i(x_i, y_i, z_i) = A_i \sin\left(\omega t + \underbrace{kx_i + ly_i + mz_i + \varphi}_{=\theta_i}\right),\ i = 1,2.$
Based on the harmonic analysis, we derive A_i, ω, and θ_i. For simplicity reasons, let us assume that $y_i = 0,\ i = 1,2$:
Then, it holds $\theta_1 - \theta_2 = k(x_1 - x_2) + m(z_1 - z_2)$. As long as z_1 is approximately equal to z_2, the z-component will not influence the derived horizontal wavelength.

The other is changing the background wind needed to calculate the intrinsic frequency because the wind is averaged at airglow altitude. This error depends on the magnitude of the vertical wind shear.

The radar data are averaged over 1 h and 4 km. We took values which are ascribed to 86 km height (+/- 2 km). I understand the reviewer question in the following way: the OH-airglow altitude can be changed by tides. It can happen that it significantly disagrees from 86 km. In this case, we have used the wrong wind. This error depends on the vertical wind shear.

According to Zhao et al. (2015), strong tidal perturbations lead to airglow-altitude changes from typically 2–7 km (referring to an observation time of 10 h at maximum). When the forcing was significantly reduced or complex in nature, no systematic trends were detected.
As long as the height changes are still within the altitude bin of 86 km, I argue that we can neglect them. The situation changes, when the changes of the OH-airglow altitude are larger. Since our height bins are 4 km, we are one bin off in this case at maximum. Placke et al. (2011) show histograms of the zonal and meridional wind shear values (prevailing and tidal wind) for the years 2005–2009 referring to July measured by the radar at Collm, which we used in our publication, too. On average, the zonal (meridional) wind shear is ca. 5 m/s/km (0 m/s/km). So, if we are one bin off, this is equivalent to 20 m/s. This agrees with the error we assumed for each wind component.

If the authors do not plan to address these issues in the analysis, they should at least be discussed.
At the end of section 3.2 (error estimation) I included the following paragraph. It consists of the arguments given in this and the previous review concerning possible tidal effects.
“Errors which may arise due to tidal effects on the OH-layer height are not considered here. Strong tidal perturbations lead to airglow-altitude changes from typically 2–7 km (Zhao et al., 2005). If all four FoV are affected to the same extent (the OH-airglow altitude is shifted by a constant value), our results are not influenced. If the OH-airglow layer height increases or decreases for each FoV individually, the derived horizontal wavelengths can change. However, our results rely on spatial and temporal averages. The FoV cover 880 km² (560 km²); all values which we derive are averaged over this area. Furthermore, we analyze time series of 7 h and longer. So, effects of motions of these scales cancel out. The four FoV are rather near to each other. This reduces the possible effect of large scale motions like tides on our analysis results tremendously. Due to the redundancy of the system (we get four values for the horizontal wavelength), we dismiss results which do not agree sufficiently (as mentioned in section 3.1). This might be the case when not all but only one or two FoV are influenced by a higher or lower airglow altitude.
There is a secondary tidal effect. If the OH-airglow layer height disagrees significantly from 86 km, we use the wind information of the wrong altitude bin. Due to the width of the altitude bins, we might be one bin off in the case of strong tidal perturbations as mentioned above. The error depends on the vertical wind shear. Placke et al. (2011) show histograms of the zonal and meridional wind shear values (prevailing and tidal wind) for the years 2005–2009 referring to July measured by the radar at Collm. On average, the zonal (meridional) wind shear is ca. 5 m/s/km (0 m/s/km). So, if we are one bin off, this is equivalent to 20 m/s. This agrees with the error which we assumed for each wind component.”

About the SABER data:
The deficiency in using SABER data to derive vertical wavelength is real and I presented the reason. The authors' arguments such as, if that's the case, then 'I can never use data ...' or 'I can expand this ... to every instrument' are missing the point, and are not a scientific argument. My point is, deriving vertical wavelength from a snapshot of a vertical profile has its limitation, and authors should be aware of it. This is obvious in authors' own analysis process, in which different approaches give different results, and they have to pick what's most favorable. The main message here is that this comparison can neither validate, nor invalidate the vertical wavelength derived from OH data. Consequently, whether the derived OH vertical wavelength agrees or disagrees with the SABER data is really not meaningful, because both have uncertainties due to different reasons and the uncertainties are as large as their differences. Again, it is OK for making the comparison just for reference (since there is no other data to compare), but it is not a validation of the OH derived vertical wavelength.

Thanks for clarifying this point. I have the impression that we mainly have a “wording problem” here: verification (provision of objective evidence) versus validation (consistency check of the results, see also Loew, A., et al., 2017). We would like to make a consistency check but of course we are aware of the deficits due to data coverage, the sensitivity of the instrument, etc.
Since the meaning of the term validation differs from community to community, it might not be the ideal choice in any case. In the satellite community, validation is based on the use of independent measurements of different instruments (e.g. satellite-based measurement versus radiosonde-based one). This implies that they are characterized by different deficits. In order to alleviate this point, I propose to use “compare” instead of “validate”.
Therefore, I changed the beginning of paragraph 4.2 to “Vertical wavelengths derived from the scanning GRIPS are compared to vertical wavelengths extracted from TIMED-SABER temperature profiles. Therefore, we identify all nights with co-located TIMED-SABER measurements around Oberpfaffenhofen.” Furthermore, I changed the last sentence of the abstract (In order to check our results, vertical temperature profiles of TIMED-SABER (Thermosphere Ionosphere Mesosphere Energetics Dynamics, Sounding of the Atmosphere using Broadband Emission Radiometry) overpasses are analysed with respect to the dominating vertical wavelength.) to “In order to compare our results ...”.

References

Chen, C., X. Chu, A. J. McDonald, S. L. Vadas, Z. Yu, W. Fong, X. Lu (2013), Inertia-gravity waves in Antarctica: A case study using simultaneous lidar and radar measurements at McMurdo/Scott Base (77.8°S, 166.7°E), J. Geophys. Res. Atmos., 118, 2794-2808.

Hu, X., A. Z. Liu, C. S. Gardner, G. R. Swenson (2002), Characteristics of quasi-monochromatic gravity waves observed with lidar in the mesopause region at Starfire Optical Range, NM, Geophys. Res. Lett., 29, 2169.

Lu, X., A. Z. Liu, G. R. Swenson, T. Li, T. Leblanc, I. S. McDermid (2009), Gravity wave propagation and dissipation from the stratosphere to the lower thermosphere, J. Geophys. Res., 114, D11101.

Our references:

- Loew, A., et al. (2017), Validation practices for satellite-based Earth observation data across communities, Rev. Geophys., 55, 779–817, doi:10.1002/2017RG000562.
- Placke, M., Stober, G., and Jacobi, C. (2011), Gravity wave momentum fluxes in the MLT—Part I: Seasonal variation at Collm (51.3°N, 13.0°E), Journal of Atmospheric and Solar-Terrestrial Physics 73, 904–910.
- Zhao, Y., Taylor, M. J., and Chu, X. (2005), Comparison of simultaneous Na lidar and mesospheric nightglow temperature measurements and the effects of tides on the emission layer heights, J. Geophys. Res., 110, D09S07, doi:10.1029/2004JD005115.

Derivation of gravity wave intrinsic parameters and vertical wavelength using a single scanning ~~Derivation of of mesospheric gravity waves horizontal and vertical wavelengths using a scanning~~ OH(3-1) airglow spectrometer

Sabine Wüst [1*], Thomas Offenwanger [1], Carsten Schmidt[1], Michael Bittner [1,2], Christoph Jacobi [3], Gunter Stober [4], Jeng-Hwa Yee [5] , Martin G. Mlynczak [6], James M. Russell III [7]

[1]Deutsches Zentrum für Luft- und Raumfahrt, Deutsches Fernerkundungsdatenzentrum, 82234 Oberpfaffenhofen, Germany
[2]Universität Augsburg, Institut für Physik, Augsburg, Germany
[3]Universität Leipzig, Institut für Meteorologie, Leipzig, Germany
[4]Institut für Atmosphärenphysik, Kühlungsborn, Germany
[5]Applied Physics Laboratory, The Johns Hopkins University, Laurel, USA
[6]NASA Langley Research Center, Hampton, USA
[7]Center for Atmospheric Sciences, Hampton, USA

Correspondence to: Sabine Wüst (sabine.wuest@dlr.de)

Abstract

For the first time, we present an approach to derive zonal, meridional and vertical wavelengths as well as periods of gravity waves based on only one OH* spectrometer addressing one vibrational-rotational transition. Knowledge of these parameters is a precondition for the calculation of further information such as the wave group velocity vector.

OH(3-1) spectrometer measurements allow the analysis of gravity wave ground-based periods, but spatial information cannot necessarily be deduced. We use a scanning spectrometer and the harmonic analysis to derive horizontal wavelengths at the mesopause altitude above Oberpfaffenhofen (48.09°N, 11.28°E), Germany for 22 nights in 2015. Based on the approximation of the dispersion relation for gravity waves of low and medium frequencies and additional horizontal wind information, we calculate vertical wavelengths. The mesopause wind measurements nearest to Oberpfaffenhofen are conducted at Collm (51.30°N, 13.02°E), Germany, ca. 380 km northeast of Ober~~f~~pfaffenhofen, by a meteor radar.

In order to ~~check~~ compare our results, vertical temperature profiles of TIMED-SABER (Thermosphere Ionosphere Mesosphere Energetics Dynamics, Sounding of the Atmosphere using Broadband Emission Radiometry) overpasses are analysed with respect to the dominating vertical wavelength.

1 Introduction

In order to analyse atmospheric motions like gravity waves, the upper mesosphere/lower thermosphere is studied by a variety of measurement techniques: airglow spectroscopy and imaging as well as lidar systems are probably the most prominent ones in the Network for the Detection of Mesospheric Change (NDMC, https://www.wdc.dlr.de/ndmc).

Depending on the instrument and the retrieval, different techniques are sensitive ~~for~~ to different wave parameters. While lidar measurements, for example, allow the ~~derivation~~ measurement of vertical wavelengths (see, e.g., Rauthe et al., 2006, 2008; Yamashita et al., 2009; Mzé et al., 2014; Chen et al., 2016), horizontal wavelengths of ~~larger scale~~ gravity waves can be directly extracted from ~~investigated by meteor radars (Oleynikov et al., 2005, 2007). A~~airglow images (for instance, Garcia et al., 1997; Taylor et al., 2003; Paulino et al., 2011)~~ing can be used for the analysis of horizontal wavelengths of shorter scale waves. Also wave periods can be derived by these techniques, if the measurements are provided with a sufficient temporal resolution (for instance, Garcia et al., 1997; Taylor et al., 2003; Yamashita et al., 2009, Paulino et al., 2011)~~. OH-airglow spectroscopy and typical meteor radar measurements ~~however (e.g., Bittner et al., 2000; Mulligan et al., 1995), if it is based on only one vibrational OH* transition, can exclusively~~ deliver gravity wave periods (e.g., Mulligan et al., 1995; Bittner et al., 2000; Hocking, 2001; Oleynikov et al., 2005~~,~~).

Further wave parameters can be calculated if additional information is available which allows the application of the dispersion relation. Also the instrument setup can be changed in order to compute further wave parameters.

Wachter et al. (2015) show that the combination of three airglow spectrometers measuring different azimuth angles allows the ~~additional~~ derivation of horizontal wavelengths. Due to the setup of the three instruments, their fields of view (FoV) and the data analysis technique, the retrieved wavelengths lie mostly in the range of a few 100s km, the addressed wave periods range from 1 to 14 h with a maximum number of waves between 2 and 4 h. Small-scale horizontal features in the order of some kilometres to a few 100s ~~k~~m or even turbulent structures, which are observed with OH* cameras as shown by Sedlak et al. (2016) and Hannawald et al. (2016)~~. and~~ cannot be investigated based on this approach.

Schmidt et al. (2017) introduced a method to ~~additionally~~ derive vertical wavelengths from OH* spectrometer measurements by observing two vibrational transitions, OH(3-1) and OH(4-2). Following the work of von Savigny (2012), the radiation emitted by the different vibrational transitions originates from slightly different heights which are separated by a few 100 m. For approximately 40% of the wave events, a vertical wavelength can be derived which lies in the range of 5–40 km. Of course, the same approach can be applied to measurements of different airglow species peaking at different heights, for example, OH(6-2) and O_2b(0-1) which are separated by ca. 7 km.

Here, we combine the approach of Wachter at al. (2015) ~~for the first time, we present an approach to~~in order to derive ~~zonal, meridional and vertical~~horizontal wavelengths (but ~~as well as wave periods~~ based on only one OH* spectrometer~~) addressing one vibrational rotational transition and on~~ with additional information about the horizontal wind and the Brunt-Väisälä frequency and compute vertical wavelengths. Thus, every component of the wave vector is known. ~~Knowledge of the spatial wave parameters~~This is a precondition for the calculation of further information like the wave group velocity vector or the

vertical flux of horizontal wave pseudomomentum, for example (see e.g. Fritts and Alexander, 2003). However, the derivation of these values is beyond the scope of this manuscript.

~~For low- and medium-frequency waves, t~~The wave vector is related to the intrinsic wave frequency, i.e., the frequency that would be observed in a frame of reference moving with the horizontal background wind, via the Brunt-Väisälä frequency and the Coriolis parameter (dispersion equation, see equation (38) in Fritts and Alexander, 2003). Based on the work of Wachter et al. (2015), we constructed a scanning OH* spectrometer (section 2.1) which allows the derivation of periods and zonal as well as meridional wavelengths (method: section 3.1, and results: section 4.1). We then use literature values of the Brunt-Väisälä frequency (see e.g. Wüst et al., 2016, 2017b) and the nearest mesopause wind measurements which are performed by a meteor radar (section 2.3) in order to estimate the vertical wavelengths (method: sections 3.1, and results: section 4.2). The scanning spectrometer operates at Oberpfaffenhofen (48.09°N, 11.28°E), Germany, the meteor radar is deployed at Collm (51.30°N, 13.02°E), Germany, ca. 380 km northeast of Oberpfaffenhofen; specific focus is therefore put on a thorough uncertainty estimation (section 3.2). Finally, the results are compared to vertical wavelengths extracted from collocated TIMED-SABER temperature profiles (section 2.2, and 4.2).

2 Measurements and data

2.1 Infrared spectrometer GRIPS

The nightly airglow observations presented here are performed with the scanning infrared spectrometer GRIPS 14 (GRound based Infrared P-branch Spectrometer) at Oberpfaffenhofen (48.09°N, 11.28°E), Germany, July–November 2015. The instrument operates in the spectral range of 1.5 µm to 1.6 µm. Therefore, observations are only possible under (nearly) cloudless conditions. They address a height of ca. 86 km (e.g. Wüst et al., 2016; Wüst et al, 2017b).

Concerning its basic components and its data processing, GRIPS 14 is identical to the GRIPS instruments described by Schmidt et al. (2013). The technical layout of the scanning mirror is designed to result in three FoV forming an equilateral triangle (zenith angles: 30°) in the mesopause region with the fourth FoV being in the center of the triangle, in the zenith direction. The edge length of the FoV triangle amounts to 90 km. Due to the finite aperture of the GRIPS 14, each FoV covers approximately 880 km² excluding the one in the zenith direction. The latter is smaller with approximately 560 km² (see fig. 1). The instrument acquires spectra with a temporal resolution of 15 s. Thus, it is possible to get airglow spectra from four FoV in approximately one minute.

The rotational temperature derived from an individual spectrum can typically exhibit an uncertainty of ±8 K. In order to improve the signal-to-noise ratio for the intended analysis, five minute mean values are calculated for each FoV. Only comparatively good individual values are used here (individual error 4.5 K and less as in Wüst et al, 2016). The error of the five-minutes values reaches ca. 3.2 K on average with a standard deviation of 0.3 K. Additional care has been taken to ensure that the data quality of each FoV is comparable to the others by manually inspecting each night: due to the geographic location of Oberpfaffenhofen just north of the Alps, it frequently happens that clouds form predominantly in the southern FoV or that the moon passes through just one of the FoV. These cases are excluded from further analysis.

2.2 TIMED-SABER

On 7th December 2001, the TIMED satellite was launched. Soon, the on-board limb-sounder SABER started to deliver vertical profiles of kinetic temperature on a routine basis. The profiles cover the height range from approximately 10 km to more than 100 km. The vertical resolution is ca. 2 km (Mertens et al., 2004; Mlynczak, 1997) which is suitable for the investigation of gravity wave activity. On a given day, the latitudinal coverage extends from about 52° latitude in one hemisphere to 83° in the other (Russell et al., 1999). This viewing geometry alternates once every 60 days due to 180° yaw manoeuvers of the TIMED satellite (Russell et al., 1999). In total, approximately 1200 temperature profiles are available per day. An overview of the large number of SABER publications is available at http://saber.gats-inc.com/publications.php.

Measurements of infrared emission from carbon dioxide in the 15 µm spectral interval are used in the SABER temperature retrieval. It is based on a comprehensive forward radiance model incorporating dozens of vibration-rotation bands of CO_2, including isotopic and hot bands, and solving the full set of coupled radiative transfer equations under non-LTE, i.e., under conditions that depart from Local Thermodynamic Equilibrium. From the temperature retrieval version 1.03 on, NLTE

algorithms for kinetic temperature were employed (López-Puertas et al., 2004; Mertens et al., 2004, 2008). This is certainly one of the main challenges for CO_2 based temperature retrievals in the mesosphere and upper levels. Comparisons with reference data sets generally confirm good quality of SABER temperatures (Remsberg et al., 2008).

We use nightly TIMED-SABER temperature data between 45.4°N and 50.8°N and 8.6°E and 14.0°E (~300 km distance from Oberpfaffenhofen (48.09°N, 11.28°N)) in its latest version (2.0). They were downloaded from the SABER homepage (saber.gats-inc.com). The exact time can be looked up in table 1. Only SABER profiles which were measured at the same time as GRIPS data series were used.

The data were detrended between 100 km and their height minimum using an iterative cubic spline approach as it is described in Wüst et al. (2017a) with a distance of 10 km between two spline sampling points. This results in a maximal detectable wavelength of 20 km (in the detrended data series). We restrict further analysis to a relatively small height interval of 60—80 km which is just below the height range addressed by GRIPS. This is due to the following reasons. Especially during summer (May–August), a time period which is also covered in this study, the mesopause is low and reaches ca. 86 km ± 3 km (von Zahn et al., 1996; She et al., 2000). Sharply changing temperature gradients are always a challenge for a de-trending procedure and artificial signals in the detrended data cannot be excluded here. This is the reason why we investigate only heights below 80 km with the harmonic analysis. The majority of commonly-used spectral analysis techniques like the fast fourier transform, the maximum entropy method and also the harmonic analysis approach, all assume the waves are stationary and therefore a constant wave amplitude. Alternative analyses suited for non-stationary time series like, for example, the wavelet analysis often suffer from a relatively coarse spectral resolution. Therefore, we restrict our analysis to the smallest possible height interval which is equal to the maximal wavelength detectable in the detrended data series.

2.3 Meteor wind radar

The VHF SKiYMET meteor radar located at Collm has been operated nearly continuously since July 2004 (Jacobi et al., 2007, 2009). It measures winds, temperatures, and some meteor parameters at altitudes between approximately 80 and 100 km. ~~The radar uses the Doppler shift of the reflected radio wave from ionized meteor trails to obtain radial velocities along the line of sight of the radio wave.~~

The radar operates at a frequency of 36.2 MHz, with 15 kW peak power at a pulse repetition frequency of 625 Hz. The transmit antenna is a crossed dipole one, while the 5 receiving antennas during 2015 were 2-element Yagi antennas, forming an interferometer to detect the meteor position.

The radar uses the Doppler shift of the reflected radio wave from ionized meteor trails to obtain radial velocities along the line of sight of the radio wave. ~~The radar delivers h~~Hourly mean horizontal wind values are obtained from a least squares fit of the ~~through~~ projection of the horizontal hourly wind components to ~~the~~ all individual radial winds within one hour and within a defined height gate under the assumption that vertical winds are small. We used height gates of 4 km width for the fit, without weighting the individual meteors and assuming that the wind field within the time-height bin is homogeneous. Horizontal homogeneity of the horizontal wind field within the radar observation volume is also assumed. The procedure is

described in Hocking et al. (2001). ~~We used height gates of 3 km width for the fit.~~ A more recent version of the wind fitting technique and error estimation of meteor radar winds can be found in Stober et al. (2017).

In order to estimate the error that arises from using the Collm observations for the wind field over Oberpfaffenhofen at a distance of about 380 km, we evaluated the differences of winds measured by the Collm radar and the 53.5 MHz OSWIN VHF radar (Latteck et al., 1999) at Kühlungsborn (54.1°N, 11.8°E), about 330 km distance from Collm, during a half-year campaign in 2004/05 (Viehweg, 2006). The OSWIN radar had been operated as a meteor radar (Singer at al., 2003), with the same analysis procedure than applied at Collm. The Collm-Kühlungsborn differences were increasing from -0.7 ± 22.3 m/s at 85 km to -2.5 ± 25.5 m/s at 94 km for the zonal component, and -0.1 ± 20.3 m/s at 85 km to -2.05 ± 24.9 m/s at 94 km for the meridional component. The small biases may be explained by the mean northward gradients of the horizontal winds, which in winter at these heights are positive for both the zonal and meridional wind components. The standard deviation is owing to waves, turbulence, and uncertainties of both systems.

Therefore, when using Collm data for estimating winds over Oberpfaffenhofen, the standard deviation of about 20 m/s may be considered as a good guess for the dynamically induced wind differences.

3 Analysis methods

3.1 Derivation of 3D wave vector

The basic idea of the algorithm applied here for the calculation of horizontal wavelengths from a scanning GRIPS instrument is already mentioned in Wachter et al. (2015). In contrast to their publication, we derive OH-temperatures for four instead of three FoV with one scanning GRIPS instrument instead of three individual (non-scanning) ones. Since three FoV are sufficient for the calculation of horizontal wavelengths, we use the additional information for the estimation of uncertainty intervals.

We apply the harmonic analysis (all-step mode, see for example Bittner et al. (1994) or Wüst and Bittner (2006)) to the four nightly time series and search for four identical (ground-based, not intrinsic) periods throughout the entire night. Further analysis steps are restricted to results which are characterized by a period longer (shorter) than 60 min (the measurement time) and an amplitude larger than or equal to 1 K. This is in accordance with the approach and the results of Wachter et al. (2015) (see their section 2.2).

Since four different triangles can be derived from four different FoV, we apply the algorithm described in Wachter et al. (2015) to each possible triangle combination. So, we get information about the horizontal wavelengths λ_h (wave numbers k_h) from each of the four triangle combinations for four waves at maximum. Zonal and meridional wavelengths (numbers) λ_x (k) and λ_y (l), phase velocities, and propagation directions can be derived. The mean parameters are calculated for each wave, and the mean absolute difference between the individual values and the mean parameters are taken as a measure of uncertainty.

Since phase velocities reported in the literature do not in most cases exceed 150 m/s (e.g., Nakamura et al., 1999; Taylor et al., 2009; Tang et al., 2014; Wachter et al., 2015), only waves with a mean phase velocity of 150 m/s at maximum and a mean horizontal wavelength of less than or equal to 3600 km are subject of further analysis. Additionally, a maximal difference of 90° between the four different wave vectors is accepted. It turned out that this criterion is the strictest one: if it is fulfilled, the others are met as well.

Going one step further than Wachter et al. (2015), we then use the dispersion relation for the estimation of vertical wavelengths. According to linear theory (see, for example, Fritts and Alexander, 2003), it holds:

$$m^2 = \frac{(k^2 + l^2)(N^2 - \sigma^2)}{(\sigma^2 - f^2)} - \frac{1}{4H^2} \quad (1)$$

where

m is the vertical wave number,

N is the Brunt-Väisälä frequency,

$\sigma = \omega - k\bar{u} - l\bar{v}$ is the intrinsic frequency (the frequency that would be observed in a frame of reference moving with the background wind $(\bar{u}, \bar{v})$),

ω is the frequency derived by the harmonic analysis,

$f = 2 \cdot \frac{2\pi}{86164\,s} \cdot \sin\beta$ is the Coriolis parameter with respect to the latitude β, which reaches typically $10^{-4}\,s^{-1}$ for mid-latitudes, and

H is the density scale height.

For low- and medium-frequency waves ($\sigma \sim f$ or $N \gg \sigma \gg f$) the dispersion relation simplifies to

$$\lambda_z = \frac{2 \cdot \pi \cdot \sqrt{\sigma^2 - f^2}}{N \cdot k_h} = \frac{2 \cdot \pi \cdot \sqrt{(\omega - k \cdot u - l \cdot v)^2 - f^2}}{N \cdot k_h} \quad (2)$$

where k_h is the horizontal wave number (see formula (38) in Fritts and Alexander, 2003). The term $\frac{1}{4H^2}$ can be neglected since it is small compared to the squared vertical wave number. Due to the selection criteria for frequency and horizontal wave numbers, ω, k, and l are rather small and the use of this approximation is justifiable.

Information about mesopause wind velocities above Oberpfaffenhofen is not available. Since tides, which are variable from day to day, play an important role in this height range, we do not rely on climatological wind values but make use of wind measurements performed with the wind meteor radar at Collm in order to estimate the intrinsic frequency.

Since GRIPS only measures the temperature at about 86 km height, but not the temperature gradient, the Brunt-Väisälä (angular) frequency is calculated based on the collocated TIMED-SABER measurements.

3.2 Error estimation

Since ω is calculated using four different time series and applying a variety of quality criteria, we argue that the error of ω is negligible. Following error propagation, the error of λ_z then sums up to

$$\Delta\lambda_z = \sqrt{\left(\frac{\partial\lambda_z}{\partial k}\Delta k\right)^2 + \left(\frac{\partial\lambda_z}{\partial l}\Delta l\right)^2 + \left(\frac{\partial\lambda_z}{\partial N}\Delta N\right)^2 + \left(\frac{\partial\lambda_z}{\partial u}\Delta u\right)^2 + \left(\frac{\partial\lambda_z}{\partial v}\Delta v\right)^2} \quad (3)$$

with

$$\frac{\partial\lambda_z}{\partial k}\Delta k = -\lambda_z \cdot \Delta k \cdot \left(\frac{\sigma \cdot u}{\sigma^2 - f^2} + \frac{k}{k^2 + l^2}\right) \quad (4)$$

$$\frac{\partial\lambda_z}{\partial l}\Delta l = -\lambda_z \cdot \Delta l \cdot \left(\frac{\sigma \cdot v}{\sigma^2 - f^2} + \frac{l}{k^2 + l^2}\right) \quad (5)$$

$$\frac{\partial\lambda_z}{\partial N}\Delta N = -\lambda_z \cdot \frac{\Delta N}{N} \quad (6)$$

$$\frac{\partial \lambda_z}{\partial u}\Delta u = -\lambda_z \cdot \frac{\sigma \cdot k}{\sigma^2 - f^2} \cdot \Delta u \quad (7)$$

$$\frac{\partial \lambda_z}{\partial v}\Delta v = -\lambda_z \cdot \frac{\sigma \cdot l}{\sigma^2 - f^2} \cdot \Delta v \quad (8)$$

Following Wüst et al. (2016) and Wüst et al. (2017b), $\frac{\Delta N}{N}$ is ca. 10%. This might be ~~too conservative~~overestimated, since N is calculated from collocated TIMED-SABER profiles. However, the satellite-based measurements do not agree exactly in space with the GRIPS measurements. They represent only a snapshot and analyses concerning the general temporal and spatial variability of N within 300 km are difficult due to the distance of individual TIMED-SABER profiles. Δu and Δv are approximately 20 m/s (see section 2.3), and Δk and Δl are estimated as stated above (see section 3.1). Now, $\Delta\lambda_z$can be calculated.

Errors which may arise due to tidal effects on the OH-layer height are not considered here. Strong tidal perturbations lead to airglow-altitude changes from typically 2–7 km (Zhao et al., 2005). If all four FoV are affected to the same extent (the OH-airglow altitude is shifted by a constant value), our results are not influenced. If the OH-airglow layer height increases or decreases for each FoV individually, the derived horizontal wavelengths can change. However, our results rely on spatial and temporal averages. The FoV cover 880 km² (560 km²); all values which we derive are averaged over this area. Furthermore, we analyze time series of 7 h and longer. So, effects of motions of these scales cancel out. The four FoV are rather near to each other. This reduces the possible effect of large scale motions like tides on our analysis results tremendously. Due to the redundancy of the system (we get four values for the horizontal wavelength), we dismiss results which do not agree sufficiently (as mentioned in section 3.1). This might be the case when not all but only one or two FoV are influenced by a higher or lower airglow altitude.

There is a secondary tidal effect. If the OH-airglow layer height disagrees significantly from 86 km, we use the wind information of the wrong altitude bin. Due to the width of the altitude bins, we might be one bin off in the case of strong tidal perturbations as mentioned above. The error depends on the vertical wind shear. Placke et al. (2011) show histograms of the zonal and meridional wind shear values (prevailing and tidal wind) for the years 2005–2009 referring to July measured by the radar at Collm. On average, the zonal (meridional) wind shear is ca. 5 m/s/km (0 m/s/km). So, if we are one bin off, this is equivalent to 20 m/s. This agrees with the error which we assumed for each wind component.

Formatiert: Schriftartfarbe: Automatisch

Formatiert: Schriftartfarbe: Text 1

Formatiert: Schriftartfarbe: Text 1

Formatiert: Englisch (USA)

4 Results and discussion

4.1 Horizontal parameters

Due to the rather strict quality criteria, horizontal wavelengths for 31 wave events in only 22 nights can be identified during the measurement period. For the majority of cases, the horizontal wavelength is shorter than 1000 km, with a maximum of the distribution between 600 and 800 km (fig. 2a). The phase velocity (relative to the ground) reaches 140 m/s at maximum and ranges mostly between 20 and 40 m/s (fig. 2b). A preferred propagation direction cannot easily be identified (fig. 2c). The data cover the time period from July to November; since the propagation direction is supposed to show seasonal variations (see Wachter et al. (2015), and references therein) and our data base is rather small, a conclusive picture cannot be drawn here.

The values for the different parameters agree well with literature. Phase velocities up to 80–100 m/s are reported, for example, by Nakamura et al. (1999), Suzuki et al. (2004), and Taylor et al. (2009). Tang et al. (2014) and Wachter et al. (2015), e.g., find horizontal phase speeds of up to 160–180 m/s. The horizontal wavelengths cannot easily be compared since many authors focus on smaller horizontal scales (see, for example, Tang et al., 2014; Taylor et al., 2009; Hannawald et al., 2016; Sedlak et al., 2016). However, Reid (1986) presents in his fig. 6 a good overview of horizontal wavelengths measured by different techniques at various locations between 60 and 100 km height. Here, it becomes clear that horizontal wavelengths of the order of 10^3 km were already observed in earlier studies. However, in order to be careful, the results of the following subsection are separated according to the horizontal wavelength (up to 1500 km and all wavelengths, provided in brackets, if the results disagree).

Formatiert: Englisch (Großbritannien)

4.2 Vertical wavelengths

~~Since TIMED-SABER temperature profiles are used for validating the v~~Vertical wavelengths derived from the scanning GRIPS are compared to vertical wavelengths extracted from TIMED-SABER temperature profiles. Therefore, we identify all nights with co-located TIMED-SABER measurements around Oberpfaffenhofen. Depending on the orbit of TIMED, it ~~happens~~ can happen that no vertical temperature profile is suitable one day. However, ~~in some cases~~the other day also more than one profile ~~is~~ can be available. In this case, multiple nearby SABER profiles which may show different vertical wavelengths can be used for comparison. Since the wind velocity changes considerably during the night, we calculate linearly weighted wind speeds from the hourly means of the wind data according to the overflight time of TIMED. If multiple nearby SABER profiles are available, the detected wave from the airglow is combined with different wind values. This leads to different vertical wavelengths based on the GRIPS-radar combination for one night. In one case, the respective hourly-averaged wind data do not exist. Therefore, 19 horizontal wavelengths of the 31 mentioned in section 4.1 referring to 14 of 22 nights can be used for further analysis. The data availability of TIMED-SABER and meteor wind measurements allows the calculation of 48 vertical wavelengths (see table 2).

In three cases, the wavelengths are shorter than 2 km (no. 23, 30 and 32 in table 1). This does not seem to be a realistic value for a layer with a full width at half maximum of 8–9 km (see fig. 9 in Wüst et al. (2016); Wüst et al. (2017b)). Furthermore, as Trinh et al. (2015) show in their fig. 7 a, SABER is not sensitive for vertical wavelengths shorter than ~2.5 km. In five cases (twice two nearly simultaneously-measured SABER profiles), the wavelengths are rather long with ca. 38.0 km (no. 36 and 37 in table 1), 45.9 km (no. 44 and 45 in table 1) and 33.4 km (no.47 in table1). This is in principle possible and was already observed in the past (see, for example, Manson, 1990, and Stober et al., 2013) but hard to verify here since we use SABER profiles only between 60 and 80 km—see section 2.2 for an explanation. In two cases (two nearly simultaneously-measured SABER profiles), the result is imaginary (no. 42 and 43 in table 12), which means that the wave cannot propagate vertically ~~and is damped~~. We cannot verify this case either. So, 38 cases (79% of 48 vertical wavelengths) show reasonable and verifiable results.

The mean vertical wavelength derived by the combination of GRIPS and the meteor radar is 11.6 km (~~f~~fig. 3a). This agrees well with literature: Rauthe et al. (2008), for example, investigated vertical lidar temperature profiles between 1 and 105 km height recorded at Kühlungsborn (54.1°N, 11.8°E), which is located about 800 km north of Oberpfaffenhofen, with a wavelet analysis. In their fig. 5 b, they show the dominating vertical wavelength depending on month. For a maximum height of 80 km, it ranges between 13 and 15 km. Senft et al. (1991) report a similar finding for Urbana (40.1°N, 88.2°W), United States of America. Based on 60 nights of Na-lidar measurements, they find that characteristic vertical wavelengths vary between 8.9 and 27 km. The annual mean reaches 14.1 km, if one refers only to summer values, it is 12.7 km, winter values show a mean of 15.5 km.
The mean error following equation (3) sums up to 59% (fig. 3b). In nearly all cases, the largest contribution to the individual $\Delta\lambda_z$ is due to the wind uncertainty (formula (7) and (8)).

In order to compare the vertical wavelengths derived by GRIPS with SABER measurements, the harmonic analysis is used for searching the detrended TIMED-SABER temperature profiles for two vertical wavelengths between 2.5 km (minimal vertical wavelengths detectable in SABER measurements according to Trinh et al., 2015) and 20 km (height interval length). Two wavelengths are chosen since an inspection by eye shows at least two oscillations in the SABER profiles. The sensitivity of TIMED-SABER depends on the vertical and horizontal wavelength along the line of sight. For a wave with 12.5 km vertical wavelength, the horizontal wavelength (along the line of sight) needs to be 450 km at least, to ensure that SABER captures it with 50% and more of its original amplitude (see Trinh et al., 2015, e.g.). The horizontal wavelength along the line of sight is always larger or equal to the true horizontal wavelength. The TIMED-SABER data are therefore suitable for our purpose (compare fig. 2 a).
The two oscillations identified by the harmonic analysis explain ca. 81% (80%) of the TIMED-SABER temperature variability on average which can be judged as a good value. The oscillation which agrees best with the vertical wavelength derived from the GRIPS-radar combination is used for further comparison (this value is given in table 1). The mean

individual difference between the vertical wavelengths of both data sets then reaches ca. 2.5 km or 21% relative to the GRIPS wavelength (fig. 4a and b). The vertical wavelengths agree within the error bars in all but four cases; here, the vertical wavelengths derived from SABER are slightly smaller by 0.2–0.8 km.

We conclude that the presented approach provides reasonable results for the 3D wave vector. However, the data basis is not very large. Like other measurement techniques or approaches, also this one is sensitive to certain horizontal and vertical wavelengths: the vertical extension of the OH*-layer limits the sensitivity of the GRIPS-instrument for vertical wavelengths to a few kilometres at least (see Wüst et al., 2016 for a comprehensive overview). The sensitivity for horizontal wavelengths is determined by the distance between the different FoV (~90 km here) and their sizes (see Wüst et al. (2016) for an estimation of this effect), as well as by the quality of the data, which strongly depends on the weather: only if a phase difference unequal to zero for the individual time series can be identified, the derivation of the horizontal wave vector and subsequently of the vertical wave number is possible.

5 Summary

Using a scanning OH-spectrometer at Oberpfaffenhofen (48.09°N, 11.28°E), Germany, we derive periods and horizontal wavelengths at the mesopause which are typical for gravity waves (ca. 1–10 h, 100–1000s km). Based on the dispersion relation, additional horizontal wind information allows the calculation of vertical wavelengths. The nearest mesopause wind measurements are carried out at Collm (51.30°N, 13.02°E), Germany, approximately 380 km northeast of Oberpfaffenhofen by a meteor radar. We assume that these values are also valid for Oberpfaffenhofen within an uncertainty of ±20 m/s.

Ca. 79% of the vertical wavelengths range between 5 km and 19–20 km. These values appear reasonable compared to literature and taking into account the vertical extension of the OH-layer. In three cases (ca. 6%), the values are not plausible.

The results are compared to vertical wavelengths derived from collocated detrended TIMED-SABER measurements. Although the spectrometer and the meteor radar are deployed about 380 km apart from each other, the vertical wavelengths based on the spectrometer-radar data combination and the satellite data only show a mean difference of 2.5 km or 21% (relative to the GRIPS wavelength). We conclude that the presented combination of measurements provides a good estimate of the vertical wavelengths on average.

Acknowledgement

We thank the Bavarian State Ministry of the Environment and Consumer Protection (BayStMinUV, VAO-project LUDWIG, TP I/3, project number TUS01 UFS-67093) and the German Ministry for Education and Research (BMBF, Grant agreement No: 01LG1206A) for funding.

Furthermore, we thank Ricarda Linz, formerly at DLR, for detrending the SABER data and Paul Wachter, DLR, for a preliminary setup of the scanning GRIPS-instrument.

Processing and long-term archiving of the data is provided by the World Data Center for Remote Sensing of the Atmosphere (WDC-RSAT, http://wdc.dlr.de). The measurements are part of the Network for the Detection of Mesospheric Change, NDMC (https://www.wdc.dlr.de/ndmc).

References

Bittner, M., Offermann, D., Bugaeva, I. V., Kokin, G. A., Koshelkov, J. P., Krivolutsky, A., Tarasenko, D. A., Gil-Ojeda, M., Hauchecorne, A., Lübken, F.-J., de la Morena, B. A., Mourier, A., Nakane, H., Oyama, K. I., Schmidlin, F. J., Soule, I., Thomas, L., and Tsuda, T.: Long period/large scale oscillations of temperature during the DYANA campaign, J. Atmos. Terr. Phys., 56, 1675–1700, doi: 10.1016/0021-9169(94)90004-3, 1994.

Bittner, M., Offermann, D., and Graef, H.-H.: Mesopause temperature variability above a midlatitude station in Europe, J. Geophys. Res., 105, 2045–2058, 2000.

Chen, C., Chu, X., Zhao, J., Roberts, B. R., Yu, Z., Fong, W., Lu, X., and Smith, J. A.; Lidar observations of persistent gravity waves with periods of 3–10 h in the Antarctic middle and upper atmosphere at McMurdo (77.83°S, 166.67°E). J. Geophys. Res.: Space Phys. 121, 1483–1502Committee on Space Research, NASA National Space Science Data Center: COSPAR International Reference Atmosphere (CIRA-86): Global Climatology of Atmospheric Parameters. NCAS British Atmospheric Data Centre, 13.03.2017, http://catalogue.ceda.ac.uk/uuid/4996e5b2f53ce0b1f2072adadaeda262, 2006.

Fritts, D. C., and Alexander, M. J.: Gravity wave dynamics and effects in the middle atmosphere, Rev. Geophys., 41, 1003, doi: 10.1029/2001RG000106, 2003.

Garcia, F.J., Taylor, M.J., and Kelly, M.C.: Two-dimensional spectral analysis of mesospheric airglow image data, Appl. Opt., 36, 7374–7385.doi: 10.1364/AO.36.007374, 1997.

Hannawald, P., Schmidt, C., Wüst, S., and Bittner, M.: A fast SWIR imager for observations of transient features in OH airglow, Atmos. Meas. Tech., 9, 1461–1472, doi:10.5194/amt-9-1461-2016, 2016.

Hocking, W.K., Fuller, B., and Vandepeer, B.: Real-time determination of meteor-related parameters utilizing modern digital technology, J. Atmos. Sol.-Terr. Phys., 63, 155–169, 2001, doi: 10.1016/S1364-6826(00)00138-3, 2001.

Jacobi, Ch., Fröhlich, K., Viehweg, C., Stober, G., and Kürschner, D.: Midlatitude mesosphere/lower thermosphere meridional winds and temperatures measured with Meteor Radar, Adv. Space Res., 39, 1278–1283, doi:10.1016/j.asr.2007.01.003, 2007.

Jacobi, Ch., Arras, C., Kürschner, D., Singer, W., Hoffmann, P., and Keuer, D.: Comparison of mesopause region meteor radar winds, medium frequency radar winds and low frequency drifts over Germany, Adv. Space. Res., 43, 247-252, doi: 10.1016/j.asr.2008.05.009, 2009.

Latteck, R., Singer, W. and Höffner, J.: Mesosphere Summer Echoes as observed by VHF Radar at Kühlungsborn 54°N, Geophys. Res. Lett., 26, 1533–1536, doi: 10.1029/1999GL900225, 1999.

López-Puertas, M., Garcia-Comas, M., Funke, B., Picard, R. H., Winick, J. R., Wintersteiner, P. P., Mlynczak, M. G., Mertens, C. J., Russell III, J. M., and Gordley, L. L.: Evidence for an OH(v) excitation mechanism of CO_2 4.3 μm nighttime emission from SABER/TIMED measurements, J. Geophys. Res., 109, D09307, doi: 10.1029/2003JD004383, 2004.

Mertens, C. J., Schmidlin, F. J., Goldberg, R.A., Remsberg, E. E., Pesnell, W. D., Russell III, J. M., Mlynczak, M. G., López-Puertas, M., Wintersteiner, P. P., Picard, R. H., Winick, J. R., and Gordley, L. L.: SABER observations of mesospheric temperatures and comparisons with falling sphere measurements taken during the 2002 summer MaCWAVE campaign, Geophys. Res. Lett., 31, L03105, doi: 10.1029/2003GL018605, 2004.

Mertens, C. J., Fernandez, J. R., Xu, X., Evans, D. S., Mlynczak, M. G., and Russell III, J. M.: A new source of auroral infrared emission observed by TIMED/SABER, Geophys. Res. Lett., 35, 17–20, doi: 10.1029/2008GL034701, 2008.

Mlynczak, M. G.: Energetics of the mesosphere and lower thermosphere and the SABER experiment, Adv. Space Res., 20, 1177–1183, doi: 10.1016/S0273-1177(97)00769-2, 1997.

Mulligan, F.J., Horgan, D.F., Galligan, J.G., and Griffin, E.M.: Mesopause temperatures and integrated band brightnesses calculated from airglow OH emissions recorded at Maynooth (53.2°N, 6.4°W) during 1993, J. Atmos. Terr. Phys., 57, 1623–1637, 1995.

Mzé, N., Hauchecorne, A., Keckhut, P., and Thétis, M.: Vertical distribution of gravity wave potential energy from long-term Rayleigh lidar data at a northern middle latitude site, J. Geophys. Res., 119, 12,069–12,083, doi: 10.1002/2014JD022035, 2014.

Nakamura, T., Higashikawa, A., Tsuda, T., and Matsushita, Y.: Seasonal variations of Gravity wave structures in OH airglow with a CCD imager at Shigaraki, Earth Planets Space, 51, 897–906, doi: 10.1186/BF03353248, 1999.

Oleynikov, A. N., Jacobi, C., and Sosnovchick, D.M.: Parameters of internal gravity waves in the mesosphere-lower thermosphere region derived from meteor radar wind measurements, Ann. Geophys., 23, 3431-3437, 2005.

~~Oleynikov, A. N., Sosnovchik, D. M., Kukush, V. D., Jacobi, C., and Fröhlich, K.: Seasonal variation of space time parameters of internal gravity waves at Kharkiv (49°30'N, 36°51'E), J. Atmos. Sol. Terr. Phys., 69, 2257–2264, doi:10.1016/j.jastp.2007.07.009, 2007.~~

Paulino, I., Takahashi, H., Medeiros, A.F., Wrasse, C.M., Buriti, R.A., Sobral, J.H.A. and Gobbi, D.: Mesospheric gravity waves and ionospheric plasma bubbles observed dur- ing the COPEX campaign, J. Atmos. Sol.-Terr. Phys., 73, 1575–1580, 2011.

Placke, M., Stober, G., and Jacobi, C.: Gravity wave momentum fluxes in the MLT—Part I: Seasonal variation at Collm (51.3°N, 13.0°E), J. Atmos. Sol.-Terr. Phys., 73, 904–910, 2011.

Rauthe, M., Gerding, M., Höffner, J., and Lübken, F.-J.: Lidar temperature measurements of gravity waves over Kühlungsborn (54°N) from 1 to 105 km: A winter-summer comparison, J. Geophys. Res., 111, D24108, doi:10.1029/2006JD007354, 2006.

Rauthe, M., Gerding, M., and Lübken, F.-J.: Seasonal changes in gravity wave activity measured by lidars at mid-latitudes, Atmos. Chem. Phys., 8, 6775–6787, doi: 10.5194/acp-8-6775-2008/, 2008.

Reid, I. M.: Gravity wave motions in the upper middle atmosphere (60–110 km), J. Atmos. Terr. Phys., 48, 1057–1072, doi: 10.1016/0021-9169(86)90026-7, 1986.

Remsberg, E. E., Marshall, B. T., Garcia-Comas, M., Krueger, D., Lingenfelser, G. S., Martin-Torres, J., Mlynczak, M. G., Russell III, J. M., Smith, A. K., Zhao, Y., Brown, C., Gordley, L. L., Lopez-Gonzalez, M. J., Lopez-Puertas, M., She, C.-Y., Taylor, M. J., and Thompson, R. E.: Assessment of the quality of the version 1.07 temperature versus pressure profiles of the middle atmosphere from TIMED/SABER, J. Geophys. Res., 113, D17101, doi: 10.1029/2008JD010013, 2008.

Russell III, J. M., Mlynczak, M. G., Gordley, L. L., Tansock Jr., J. J., and Esplin, R. W.: Overview of the SABER experiment and preliminary calibration results, Proc. SPIE 3756, P. Soc. Photo-Opt. Ins., 277-288, doi: 10.1117/12.366382, 1999.

Schmidt, C., Höppner, K., and Bittner, M.: A ground-based spectrometer equipped with an InGaAs array for routine observations of OH(3-1) rotational temperatures in the mesopause region, J. Atmos. Sol.-Terr. Phys., 102, 125–139, doi: 10.1016/j.jastp.2013.05.001, 2013.

Schmidt, C., Dunker, T., Lichtenstern, S., Scheer, J., Wüst, S., Hoppe, U.P., Bittner M.: Derivation of vertical wavelengths of gravity waves in the MLT-region from multispectral airglow observations, J. Atmos. Sol.-Terr. Phys., in review, 2017.

Sedlak, R., Hannawald, P., Schmidt, C., Wüst, S., and Bittner, M.: High-resolution observations of small-scale gravity waves and turbulence features in the OH airglow layer, Atmos. Meas. Tech., 9, 5955–5963, doi: 10.5194/amt-9-5955-2016, 2016.

Senft, D. C., and Gardner, C. S.: Seasonal variability of gravity wave activity and spectra in the mesopause region at Urbana, J. Geophys. Res., 96, 17229–17264, doi: 10.1029/91JD01662, 1991.

She, C. Y., Chen, S., Hu, Z., Sherman, J., Vance, J. D., Vasoli, V., White, M. A., Yu, J., and Krueger, D. A.: Eight-year climatology of nocturnal temperature and sodium density in the mesopause region (80 to 105 km) over Fort Collins, Co (41° N, 105° W), Geophys. Res. Lett., 27, 3289-3292, 2000.

Singer, W., Bremer, J., Hocking, W. K., Weiß, J., Latteck, R., and Zecha M.: Temperature and wind tides around the summer mesopause at middle and Arctic latitudes, Adv. Space Res., 31, 2055-2060, doi: 10.1016/S0273-1177(03)00228-X, 2003.

Stober, G., Sommer, S., Rapp, M., and Latteck, R.: Investigation of gravity waves using horizontally resolved radial velocity measurements, Atmos. Meas. Tech., 6, 2893–2905, doi: 10.5194/amt-6-2893-2013, 2013.

Stober, G., Matthias, V., Jacobi, C., Wilhelm, S., Höffner, J., and Chau, J. L.: Exceptionally strong summer-like zonal wind reversal in the upper mesosphere during winter 2015/16, Ann. Geophys., 35, 711–720, doi: 10.5194/angeo-35-711-2017, 2017.

Suzuki, S., Shiokawa, K., Otsuka, Y., Ogawa, T., and Wilkinson, P.: Statistical characteristics of gravity waves observed by an all-sky imager at Darwin, Australia, J. Geophys. Res., 109, D20S07, doi: 10.1029/2003JD004336, 2004.

Tang, Y., Dou, X., Li, T., Nakamura, T., Xue, X., Huang, C., Manson, A., Meek, C., Thorsen, D., and Avery, S.: Gravity wave characteristics in the mesopause region revealed from OH airglow imager observations over Northern Colorado, J. Geophys. Res. Space Phys., 119, 630–645, doi: 10.1002/2013JA018955, 2014.

Taylor, M. J., Pendleton Jr, W. R., Seo, S. H., and Picard, R. H.: Remote sensing of gravity wave intensity and temperature signatures at mesopause heights using the nightglow emissions, Proc. SPIE, 4882, 122–133, 2003.

Taylor, M. J., Pautet, P.-D., Medeiros, A. F., Buriti, R., Fechine, J., Fritts, D. C., Vadas, S. L., Takahashi, H., and São Sabbas, F. T.: Characteristics of mesospheric gravity waves near the magnetic equator, Brazil, during the SpreadFEx campaign, Ann. Geophys., 27, 461–472, doi: 10.5194/angeo-27-461-2009, 2009.

Trinh, Q. T., Kalisch, S., Preusse, P., Chun, H.-Y., Eckermann, S. D., Ern, M., and Riese, M.: A comprehensive observational filter for satellite infrared limb sounding of gravity waves, Atmos. Meas. Tech., 8, 1491–1517, doi: 10.5194/amt-8-1491-2015, 2015.

Viehweg, C.: Statistische Analyse von Meteorradardaten, Diploma Thesis, University of Leipzig, 86 pp, 2006.

von Savigny, C., McDade, I. C., Eichmann, K. U., and Burrows, J. P.: On the dependence of the OH* Meinel emission altitude on vibrational level: SCIAMACHY observations and model simulations, Atmos. Chem. Phys., 12, 8813–8828, doi: 10.5194/10.5194/acp-12-8813-2012, 2012.

von Zahn, U., Höffner, J., Eska, V., and Alpers, M.: The mesopause altitude: Only two distinctive levels worldwide?, Geophys. Res. Lett., 23, 3231–3234, 1996.

Wachter, P., Schmidt, C., Wüst, S., and Bittner, M.: Spatial gravity wave characteristics obtained from multiple OH(3–1) airglow temperature time series, J. Atmos. Sol.-Terr. Phys., 135, 192–201, doi: 10.1016/j.jastp.2015.11.008, 2015.

Wüst, S., and Bittner, M.: Non-linear resonant wave–wave interaction (triad): Case studies based on rocket data and first application to satellite data. J. Atmos. Sol.-Terr. Phys., 68, 959–976, doi: 10.1016/j.jastp.2005.11.011, 2006.

Wüst, S., Wendt, V., Schmidt, C., Lichtenstern, S., Bittner, M., Yee, J.-H., Mlynczak, M. G., and Russell III, J. M.: Derivation of gravity wave potential energy density from NDMC measurements, J. Atmos. Sol.-Terr. Phys., 138, 32–46, doi: 10.1016/j.jastp.2015.12.003, 2016.

Wüst, S., Wendt, V., Linz, R., and Bittner, M.: Smoothing data series by means of cubic splines: quality of approximation and introduction of a repeating spline approach, Atmos. Meas. Tech., 10, 3453–3462, doi: 10.5194/amt-10-3453-2017, 2017a.

Wüst, S., Bittner, M., Yee, J.-H., Mlynczak, M. G., and Russell III, J. M.: Variability of the Brunt-Väisälä frequency at the OH*-layer height, Atmos. Meas. Tech., 10, 4895–4903, doi: 10.5194/amt-10-4895-2017, 2017b.

Yamashita, C., Chu, X., Liu, H.-L., Espy, P. J., Nott, G. J., and Huang, W.: Stratospheric gravity wave characteristics and seasonal variations observed by lidar at the South Pole and Rothera, Antarctica, J. Geophys. Res., 114, D12101, doi: 10.1029/2008JD011472, 2009.

Zhao, Y., Taylor, M. J., and Chu, X.: Comparison of simultaneous Na lidar and mesospheric nightglow temperature measurements and the effects of tides on the emission layer heights, J. Geophys. Res., 110, D09S07, doi: 10.1029/2004JD005115, 2005.

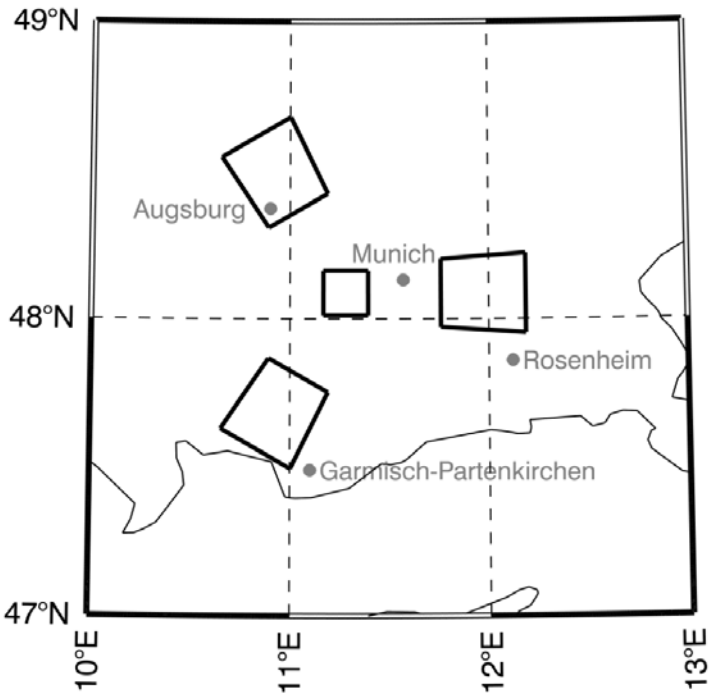

Figure 1: The scanning GRIPS points ~~at four~~ in 4 different directions. The FoV in the zenith direction is the smallest one with an edge length of 23–24 km at the mesopause height resulting in a covered area of ca. 560 km². The remaining three FoV are larger (approximately 880 km²). All four FoV together form an equilateral triangle, whose sides are approximately 90 km long.

(a)

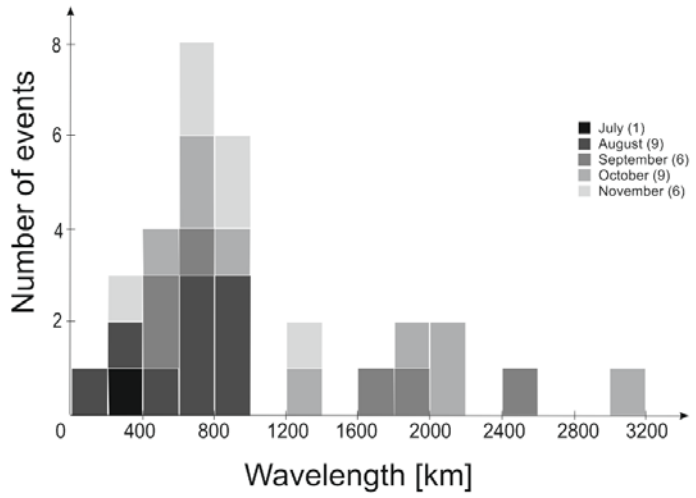
Number of events
8
6
4
2
0
400
800
1200
1600
2000
2400
2800
3200
Wavelength [km]
July (1)
August (9)
September (6)
October (9)
November (6)

(b)

(c)

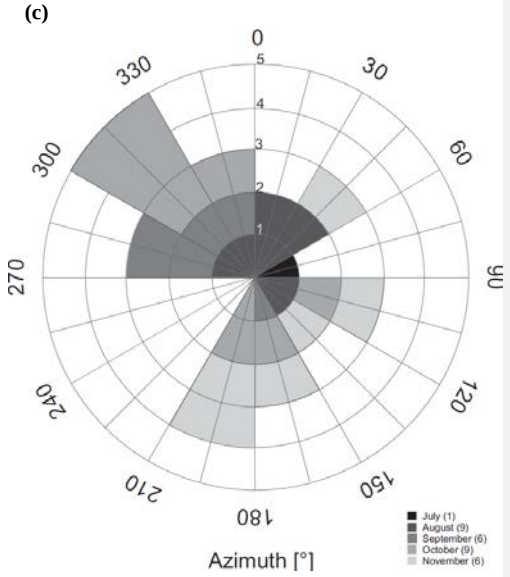
0
30
60
90
120
150
180
210
240
270
300
330
5
4
3
2
1
Azimuth [°]
July (1)
August (9)
September (6)
October (9)
November (6)

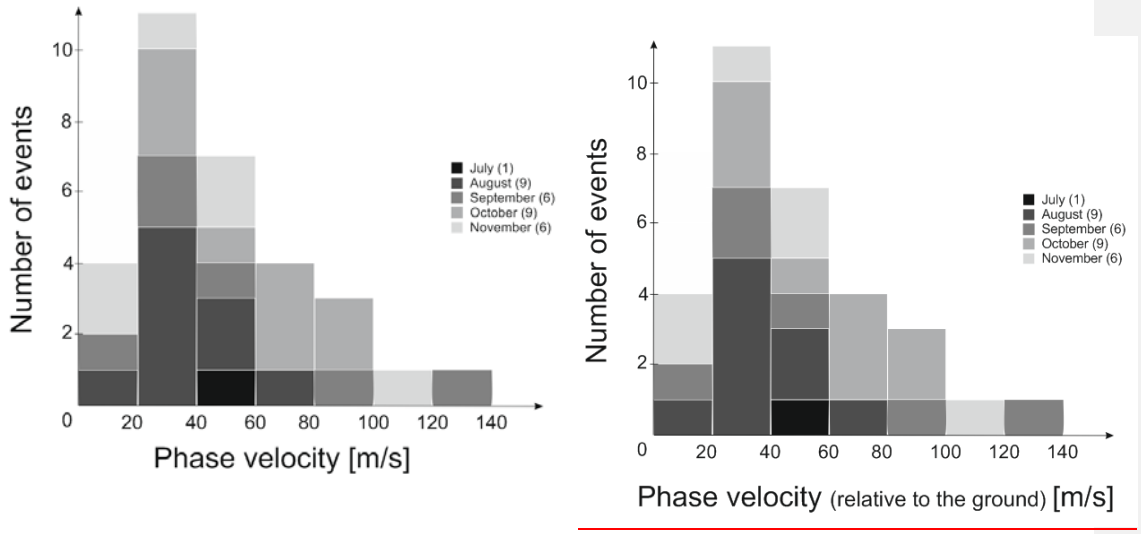

Figure 2: The histogram of the horizontal wavelengths (a) shows that the majority of detected wave events reaches up to 1000 km. The distribution of phase velocities (relative to the ground, ~~(~~b) is smoother and has a maximum between 20 and 40 m/s. The diagram of horizontal propagation directions (c) does not show a conclusive picture. The different grey colours refer to the different months.

(a)

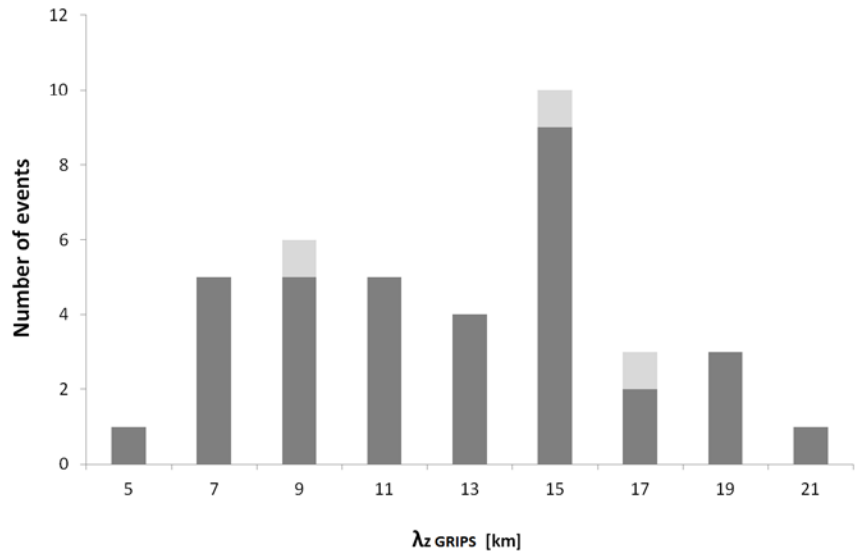
12
10
8
6
4
2
0
Number of events
5
7
9
11
13
15
17
19
21
λz GRIPS [km]

(b)

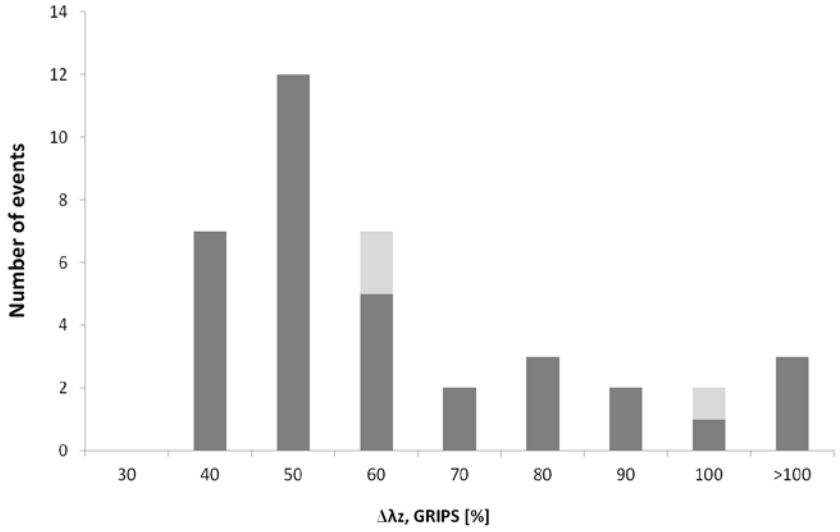
14
12
10
8
6
4
2
0
Number of events
30
40
50
60
70
80
90
100
>100
Δλz, GRIPS [%]

Figure 3 The mean calculated vertical wavelength is ca. 11.6 km, while the individual values spread from 5 km to 19–20 km (a, the x-axis labels are the upper limits of the respective intervals). The mean error of the vertical wavelength $\Delta\lambda_z$ based on error propagation calculations reaches ca. 59% (b). At minimum, it ranges between 30% and 40%; in three cases, it is more than 100%. The values for the waves with horizontal wavelengths larger than 1500 km are marked in light grey.

(a)

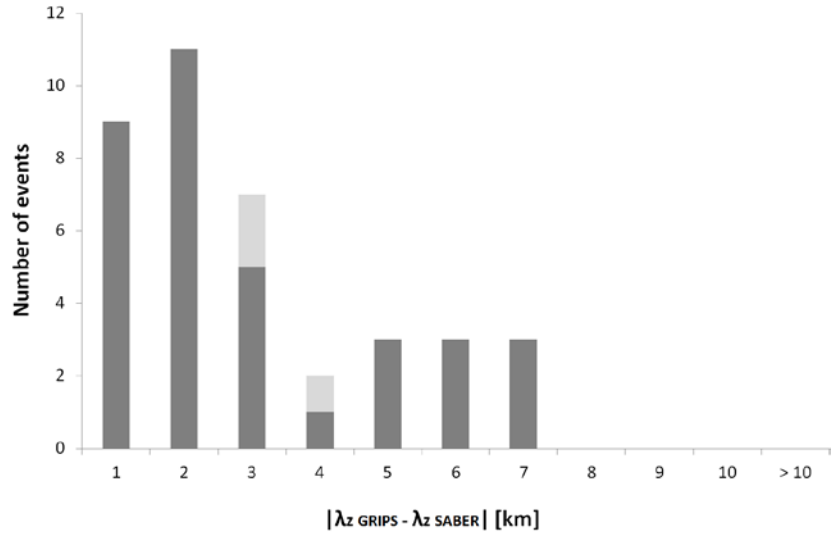

(b)

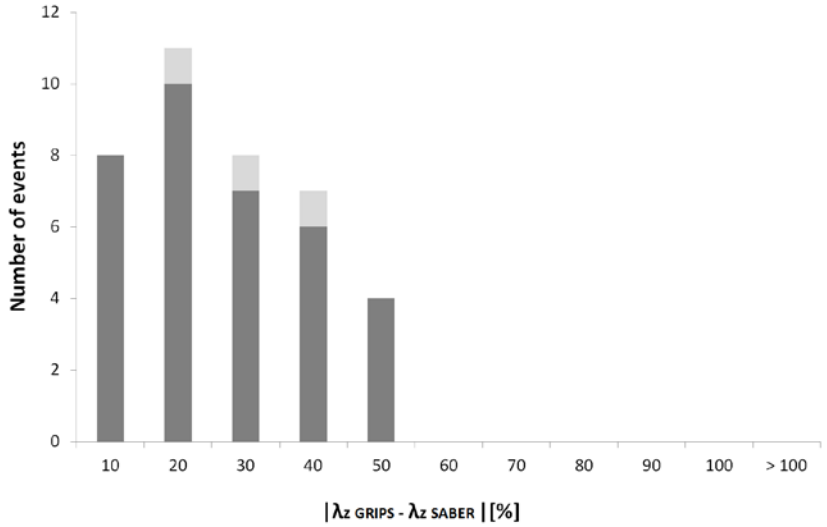

Figure 4 The mean difference between the vertical wavelength derived by the scanning GRIPS $\lambda_{z,GRIPS}$ and the most similar one identified in collocated TIMED-SABER vertical temperature profiles $\lambda_{z,SABER}$ is ca. 2.5 km (a) or 21% (b). It reaches 6–7 km or 40–50% at maximum.

Table caption

Ground-based ~~P~~period T, intrinsic frequency σ, vertical and horizontal wavelengths, λ_z and λ_h, as well as error of the vertical wavelength $\Delta\lambda_z$, derived from GRIPS, ~~as well as~~and vertical wavelength λ_z (if calculated) derived from SABER measurements during different nights (DoY = day of year when the measurement started), and date as well as time of the co-located SABER measurements.

Formatiert: Englisch (Großbritannien)

Table 1

No.	DoY GRIPS (evening)	DoY SABER	UTC SABER	Ground-based period ~~$T_{ground-based}$~~ [min]	Intrinsic period [min]	$\lambda_{h,GRIPS}$ [km]	$\lambda_{z,GRIPS}$ [km]	$\Delta\lambda_{z,GRIPS}$ [%]	$\lambda_{z,SABER}$ [km]
1	212	212	23.62	74	87	224	10.5	50	12.6
2	212	213	1.32	74	95	224	9.7	53	8.1
3	214	214	22.37	436	209	735	13.8	43	11.0
4	214	214	22.39	436	209	735	13.8	43	14.5
5	214	214	24.08	436	262	735	12.1	50	7.0
6	214	214	24.10	436	262	735	9.2	50	9.0
7	214	215	1.78	436	349	735	7.6	69	8.7
8	215	215	22.61	348	175	745	18.0	37	11.2
9	215	215	22.63	348	175	745	16.2	37	12.1
10	215	215	24.31	348	209	745	14.3	41	15.7
11	215	215	24.32	348	209	745	13.0	42	7.2
12	215	216	2.01	348	262	745	11.7	51	12.7
13	215	216	2.03	348	262	745	11.0	51	12.4
14	215	215	22.61	107	70	226	14.4	40	11.2
15	215	215	22.63	107	70	226	13.0	40	12.1
16	215	215	24.31	107	105	226	8.7	60	9.1
17	215	215	24.32	107	105	226	7.9	60	7.2
18	215	216	2.01	107	150	226	6.3	86	8.2
19	215	216	2.03	107	150	226	5.9	86	7.1
20	216	216	22.86	168	209	652	13.4	44	15.9
21	216	217	0.56	168	209	652	14.2	39	16.1
22	221	221	22.33	393	262	823	13.2	47	14.5
23	221	221	24.04	393	1047	823	1.5	---	---
24	221	221	22.33	148	131	525	19.1	36	14.5
25	221	221	24.04	148	262	525	10.8	64	8.9
26	225	225	19.88	274	262	857	15.1	38	8.7

Formatierte Tabelle ...
Formatiert ...

27	225	225	21.58	274	262	857	14.1	42	9.8
28	225	225	23.27	274	209	857	17.4	33	10.9
29	225	225	23.28	274	209	857	18.3	33	12.4
30	234	234	20.29	436	-1047	801	1.9	---	---
31	234	234	21.99	436	524	801	5.0	138	5.5
32	239	239	19.77	536	-262	81	1.3	---	---
33	239	239	21.46	536	-62	81	6.4	94	9.4
34	254	254	23.13	626	524	657	5.8	117	5.3
35	254	254	23.14	626	524	657	5.5	116	3.6
36	259	259	22.59	324	209	1691	36.6	---	---
37	259	259	22.60	324	209	1691	38.8	---	---
38	259	259	22.59	200	209	421	8.3	71	8.5
39	259	259	22.60	200	209	421	8.8	71	11.7
40	263	263	21.82	608	524	1801	15.9	51	13.8
41	263	263	21.83	608	524	1801	14.0	51	17.4
42	275	275	19.53	616	---	---	imaginary	---	---
43	275	275	19.54	616	---	---	imaginary	---	---
44	275	275	19.53	158	116	634	44.6	---	---
45	275	275	19.54	158	116	634	44.4	---	---
46	284	285	3.51	557	-349	2054	7.8	95	5.4
47	284	285	3.51	257	150	436	33.4	---	---
48	292	293	1.99	550	524	891	12.4	80	14.1